Geol. Mag. **152** (*4*), *2015, pp. 575–588.* © *Cambridge University Press 2014*
doi:10.1017/S0016756814000454

Petrography and geochemistry of the Carboniferous–Triassic Trinity Peninsula Group, West Antarctica: implications for provenance and tectonic setting

PAULA CASTILLO*‡†, JUAN PABLO LACASSIE§, CARITA AUGUSTSSON¶‖ & FRANCISCO HERVÉ‡#

*Research School of Earth Sciences, The Australian National University, Canberra ACT 0200, Australia
‡Departamento de Geología, Universidad de Chile, Plaza Ercilla 803, Santiago, Chile
§Servicio Nacional de Geología y Minería, Av. Santa María 0104, Santiago, Chile
¶Institut für Geologie und Paläontologie, Westfälische Wilhelms-Universität Münster Corrensstrasse 24, 48 149 Münster, Germany
‖Institutt for Petroleumsteknologi, Universitetet i Stavanger, 4036 Stavanger, Norway
#Escuela de Ciencias de la Tierra, Universidad Andrés Bello, Sazié 2315, Santiago, Chile

(*Received* 24 February 2014; *accepted* 17 July 2014; *first published online* 29 September 2014)

Abstract – The Carboniferous-Triassic Trinity Peninsula Group is a metasedimentary sequence that crops out widely in the northern Antarctic Peninsula. These are some of the most extensive outcrops in the area and hold the key to evaluating the connections of the Antarctic Peninsula in Gondwana; however, they are still poorly understood. Here we present our provenance study of the Trinity Peninsula Group using petrographic and geochemical approaches in combination with cathodoluminescence of detrital quartz in order to constrain its source characteristics and tectonic setting. Using differences in modal composition and quartz cathodoluminescence characteristics, we define three petrofacies derived from the progressive uplift and erosion of a volcano-plutonic continental arc, which exposed the plutonic-metamorphic roots. As indicated by major and trace elements, the source is felsic with a composition ranging from tonalitic to granodioritic. The relatively unweathered condition of the source area points to a dry and cold climate at the time of deposition, but this does not necessarily mean that it was glaciated. Deposition of the sediments occurred within an active continental margin, relatively close to the source area, probably along the south Patagonia–Antarctic Peninsula sector of Gondwana. Strong chronological, petrological and chemical similarities with the sediments of the Duque the York Complex in Patagonia suggest that they were derived from the same source.

Keywords: cathodoluminescence, detrital quartz, Palaeozoic, Gondwana, Antarctic Peninsula.

1. Introduction

The Antarctic Peninsula of West Antarctica contains some of the most extensive outcrops in Antarctica and is key to understanding the SW Pacific margin of the Gondwana supercontinent. During the break-up of Gondwana, which started in the Jurassic (König & Jökat, 2006), the Antarctic Peninsula separated from southernmost South America (Patagonia) forming the Weddell Sea. Although there are geophysical constraints on the evolution of the Weddell Sea crust (Ghidella, Yáñez & LaBrecque, 2002; König & Jökat, 2006), the relative pre-break-up position of the Antarctic Peninsula with respect to other components of Gondwana is a still matter of debate. Plate tectonic reconstructions have variably placed the Antarctic Peninsula as a straight prolongation of the Patagonian Andes or in a position parallel to Patagonia along the Pacific coast (see Miller, 2007). This debate is partly due to the poorly exposed pre-Jurassic rocks throughout the region, the difficulty of defining accurate sea floor isochrons older than 83.5 Ma (Ghidella, Yáñez & LaBrecque, 2002; Ghidella *et al.* 2007), and the remagnetization of Permo-Triassic and Jurassic rocks in the Antarctic Peninsula (Poblete *et al.* 2011). In the Antarctic Peninsula, the spatial distribution and stratigraphic relationships of different units are not well known, and large areas still do not have a stratigraphic allocation.

Upper Palaeozoic to lower Mesozoic sedimentary rocks represent some of the oldest vestiges of Gondwana in the Antarctic Peninsula. In particular, rocks from the Carboniferous-Triassic Trinity Peninsula Group (TPG) occur widely in the northern Antarctic Peninsula (Fig. 1). They have been interpreted as turbidites or debris flow deposits along an active continental margin (Hyden & Tanner, 1981; Bradshaw *et al.* 2012), which was possibly glaciated (Willan, 2003). The geological setting of the TPG is not clear. Views are conflicted between an accretionary complex (e.g. Dalziel, 1984; Storey & Garrett, 1985) and an upper slope basinal setting (Smellie, 1987, 1991; Bradshaw *et al.* 2012). The source of the TPG was probably regional and located on Western Gondwana

†Author for correspondence: paula.castillo@anu.edu.au

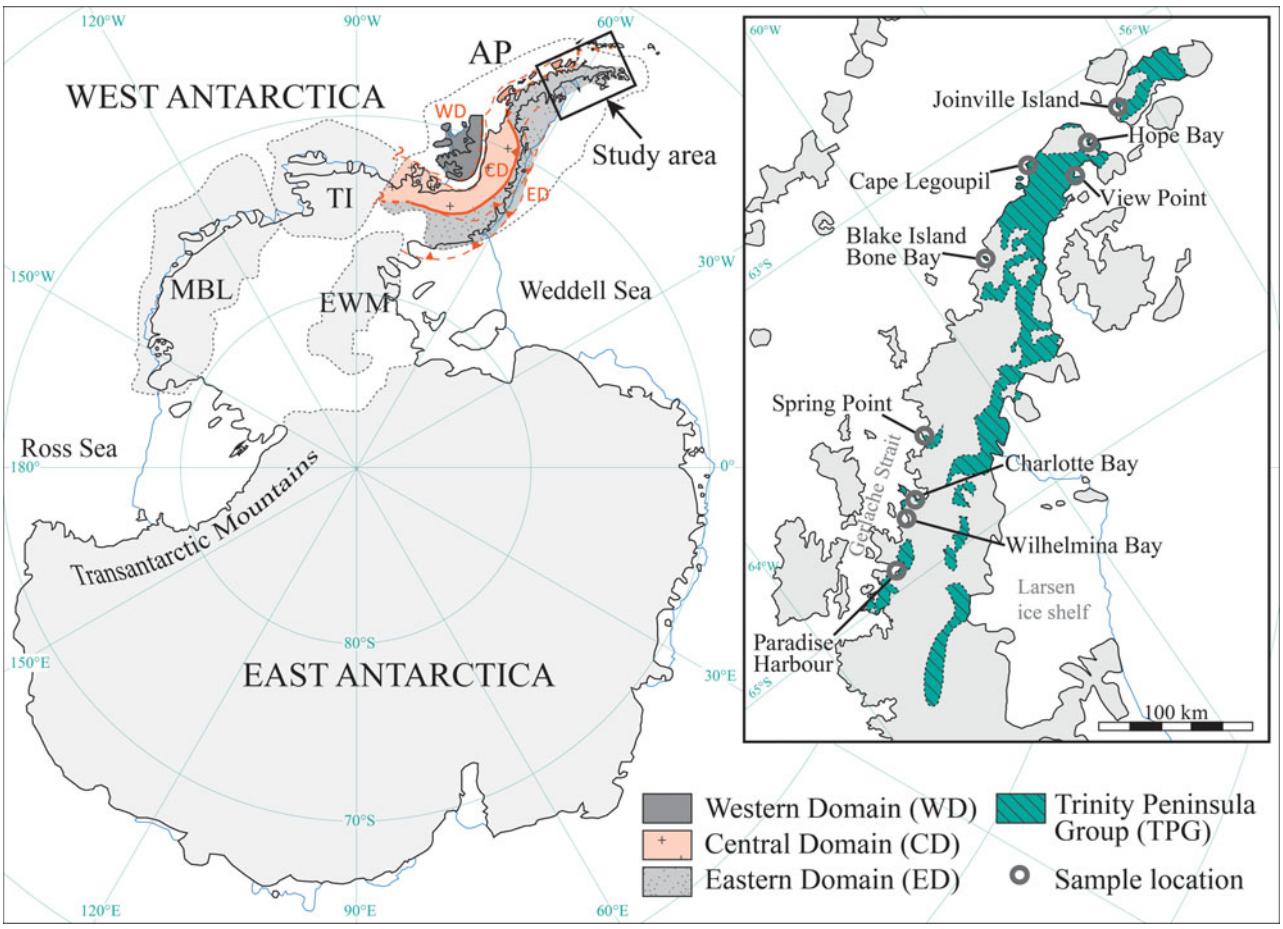

Figure 1. (Colour online) Map of localities mentioned in the text, sample location, tectonic blocks and domains. AP – Antarctic Peninsula, with domains modified after Vaughan & Storey (2000); EWM – Ellsworth-Whitmore Mountain; MBL – Marie Byrd Land; TI – Thurston Island. The insert shows a simplified geological map prepared by the British Antarctic Survey (1985).

(Barbeau *et al.* 2010), but the Northern Patagonia Massif and the Choiyoi siliceous volcanic province in South America are the most commonly suggested candidates (e.g. Willan, 2003; Fanning *et al.* 2011). Clarifying the tectonic setting and the provenance of the TPG will help us to evaluate between different models proposed for the pre-break-up position of the Antarctic Peninsula.

We present a provenance study of 24 sedimentary samples from the TPG from seven localities in the northern Antarctic Peninsula (Fig. 1). This study grants insight into the palaeogeological setting of the SW Pacific margin of Gondwana and uses different petrofacies, which are derived from the same source, to suggest the stratigraphic order of this sequence. Furthermore, we combine petrographic and geochemical whole-rock data as well as the cathodoluminescence characteristics of detrital quartz for this purpose.

2. Geological setting

The TPG is a metasedimentary sequence of Carboniferous-Triassic age which crops out in the northern Antarctic Peninsula for about 500 km (Hyden & Tanner, 1981). It probably belongs to the Eastern Domain of the Peninsula (Fig. 1), which represents the continental Gondwana margin (Vaughan & Storey, 2000). The TPG is divided into the Hope Bay, Legoupil, View Point, Bahía Charlotte and Paradise Harbour formations (Alarcón *et al.* 1976; Hyden & Tanner, 1981; Birkenmajer, 1992), which presumably overlie Palaeozoic basement orthogneiss and paragneiss (Millar, Pankhurst & Fanning, 2002; Flowerdew, 2008), but no contact relationships have been observed and the stratigraphic order between the formations is unclear. A Permian–Triassic depositional age has been assumed for most of the TPG based on detrital zircon U–Pb ages (Hervé, Miller & Pimpirev, 2005; Barbeau *et al.* 2010). Fossil evidence suggests that at least part of the TPG at Cape Legoupil is Triassic (Thomson, 1975). The View Point Formation is the only part of the TPG that may be Late Carboniferous – Early Permian in age (Bradshaw *et al.* 2012).

Metamorphism of the TPG shows an uninterrupted progression of prehnite–pumpellyite-, pumpellyite–actinolite- and greenschist-facies conditions with maximum temperatures of 300 °C to 380 °C at low to intermediate pressures (Smellie, 1991; Smellie & Millar, 1995; Smellie, Roberts & Hirons, 1996). The metamorphic grade and intensity of deformation generally increases from Hope Bay (almost unaltered mudstone and sandstone rocks) to the Nordenskjold Coast (fully

https://doi.org/10.1017/S0016756814000454 Published online by Cambridge University Press

recrystallized schists) as indicated by Smellie (1991) and Smellie, Roberts & Hirons (1996).

The provenance of the TPG has been studied using traditional petrographic tools (Smellie, 1987, 1991; Birkenmajer, 1992), whole-rock chemistry (Willan, 2003) and detrital zircon ages (Barbeau *et al.* 2010; Bradshaw *et al.* 2012). Based on sandstone petrofacies characteristics, Smellie (1987, 1991) suggested a dissected arc provenance for the Hope Bay Formation, and a mix between recycled-orogen and dissected arc types for the View Point and Legoupil formations. Low CIA values (chemical index of alteration; Nesbitt & Young, 1982) for samples from the Hope Bay, Legoupil and View Point formations suggest derivation of the detritus from a glaciated continental margin (Willan, 2003). Moreover, detrital zircon U–Pb age patterns have revealed a large proportion of Permian igneous detrital zircon grains (Hervé, Miller & Pimpirev, 2005; Barbeau *et al.* 2010; Fanning *et al.* 2011).

Based on detrital zircon U–Pb data, some authors (e.g. Barbeau *et al.* 2010; Fanning *et al.* 2011) assumed that the source of the TPG is the Permian igneous rocks from the North Patagonian Massif and the Permo-Triassic Choiyoi siliceous volcanic province in Patagonia. This interpretation is based mostly on the absence of any suitable Permian proximal source for the TPG. However, Permian magmatism and metamorphism was recently reported in the Antarctic Peninsula, providing a proximal source for the TPG (Riley, Flowerdew & Whitehouse, 2012). The Permo-Triassic Duque de York Complex (Forsythe & Mpodozis, 1983) and the Devonian–Permian Eastern Andes Metamorphic Complex (Hervé, 1993) in Patagonia have been correlated with the TPG owing to similarities in detrital zircon age patterns (Hervé, Miller & Pimpirev, 2005; Barbeau *et al*. 2010; Bradshaw *et al.* 2012).

3. Sampling and methods

Sandstone and mudstone samples from the TPG were collected from seven localities in the Antarctic Peninsula (Fig. 1). Twenty-four sandstone samples were selected for point-count analysis on the basis of their low deformation and recrystallization, ascertained from petrographic examinations. The ≥ 63 μm grain-size population of quartz, feldspar and lithic fragments were point-counted (400 in each thin-section) following the Gazzi–Dickinson method (Ingersoll *et al.* 1984). Whole-rock major and trace element concentrations of 17 sandstone and 16 mudstone samples were determined by inductively coupled plasma mass spectrometry (ICP-MS) and inductively coupled plasma atomic emission spectroscopy (ICP-AES) at ACME Labs, Canada and the Geology Department, Universidad de Chile. For all diagrams the data were normalized to 100 % on a loss-on-ignition (LOI) free basis.

Sandstone samples with cathodoluminescence (CL) colours in quartz unaffected by postdepositional metamorphism were chosen for CL investigations of detrital quartz at the Institut für Geologie und Paläontologie, Münster, Germany. We analysed a total of 358 quartz grains in 13 sandstone samples (32–68 grains/sample) in polished thin-sections coated with carbon. We used a hot-cathode luminescence microscope (HC-1LM) coupled with a water-cooled ANDOR OE-CCD detector, following procedures described in Augustsson & Reker (2012). Wavelength spectra at 375–890 nm with a resolution of ≤ 1.04 nm were measured for randomly selected quartz grains of ≥ 130 μm size, using a spot diameter of 40 μm. The system was operated at 10 kV with a sample current of *c*. 0.45 μA mm^{-2}. The spectra were measured at temperatures between −70° and −64 °C. Wavelength calibrations were made with Hg and Ar lamps. All spectra were background corrected and had measuring times of 50 s. Interval measurements of 5 × 10 s were carried out for some grains to rule out time-dependent spectral changes. We only recorded minor changes which did not exceed the range presented by Augustsson & Reker (2012). For data evaluation, we used the relative intensity of the two dominant peaks of quartz grains with respect to the position of the trough between both peaks, following the classification scheme proposed by Augustsson & Reker (2012).

4. Results

4.a. Sandstone petrography

The analysed sandstone samples are fine- to medium-grained and moderately to poorly sorted arkose (according to the classification scheme of Folk, 1980), while lithic arkose dominates at Hope Bay. Monocrystalline quartz and feldspar are the dominant components, ranging from 29 % of the total modal composition to 59 %, and 30 % to 51 %, respectively (Table 1). Plagioclase is more abundant than K-feldspar and both show varying degrees of alteration, mainly being replaced by sericite. Fresh feldspar grains usually have albite and Carlsbad twinning. Lithic fragments are less abundant, ranging from 13 % to 23 % of the total modal composition at Hope Bay and Joinville Island, and less than 13 % at other localities. Sericitized volcanic clasts are the most abundant and two types of these have been recognized: intermediate volcanic rock fragments with plagioclase and opaque mineral phenocrysts, and more commonly, very fine-grained, less altered felsic volcanic rock. Metamorphic quartzite clasts have also been recognized, especially at Charlotte and Wilhelmina bays, but they represent less than 3 % of the total modal composition of those areas.

Accessory framework minerals make up less than 2 % and include muscovite, biotite, chlorite, other heavy minerals (apatite, zircon, garnet, titanite and epidote) and opaque minerals. There is only a small variation between different samples. The matrix content is usually 5–12 % and consists of phyllosilicates (mainly smectite), which give it a black appearance. At Cape Legoupil, the matrix consists of chlorite and other phyllosilicates. Most sandstone samples contain veinlets of sericite, quartz and epidote.

https://doi.org/10.1017/S0016756814000454 Published online by Cambridge University Press

Table 1. Sandstone samples framework composition

	Sample	Q	F	L	Qm	Qp	Lt
Joinville I. (Pf A)	BR-829	37.5	40.0	22.5	34.5	3.0	25.5
Hope Bay (Pf A)	PANTI-03	35.0	48.0	17.0	33.0	2.0	19.0
	PANTI-04	34.3	44.8	21.0	31.8	2.5	23.5
	PANTI-06	43.8	43.3	13.0	42.0	1.8	14.8
	PANTI-10	57.7	30.3	12.1	53.1	4.6	16.7
	HB-03	28.5	51.0	20.5	22.0	6.5	27.0
	HB-04	31.3	48.8	20.0	28.8	2.5	22.5
	HB-05	36.8	47.8	15.5	34.8	2.0	17.5
	HB-06	34.8	50.0	15.3	31.8	3.0	18.3
	HB-07	35.8	48.5	15.8	33.5	2.3	18.0
Cape Legoupil (Pf C)	PANTI-14	54.5	39.5	6.0	51.5	3.0	9.0
	PANTI-18	54.0	36.5	9.5	52.5	1.5	11.0
	IR-01B	44.5	46.3	9.3	43.0	1.5	10.8
	IR-03B	54.0	37.0	9.0	52.5	1.5	10.5
Bone Bay (Pf B)	PANTI-2–01	53.8	40.0	6.3	51.8	2.0	8.3
Spring Point (Pf B)	PANTI-24	47.8	46.0	6.3	46.8	1.0	7.3
	PANTI-26	49.3	43.8	7.0	48.0	1.3	8.3
	PANTI-28	54.0	36.5	9.5	52.5	1.5	11.0
Wilhelmina Bay (Pf B)	AA-0842	52.0	35.5	12.5	50.5	1.5	14.0
	AA-0843	46.3	48.0	5.8	45.8	0.5	6.3
Paradise Harbour (Pf B)	PANTI-20	49.8	42.8	7.5	48.0	1.8	9.3
	PANTI-22	58.5	40.8	0.8	57.8	0.8	1.5
	PANTI-29	56.0	43.3	0.8	51.8	4.3	5.0
	PB-08A	57.0	38.8	4.3	57.0	0.0	4.3

Q:F:L – framework quartz, feldspar and lithic fragment content recalculated to 100 %
Q – total quartz (Qm + Qp); Lt – total lithic fragments (L + Qp); Pf – petrofacies.

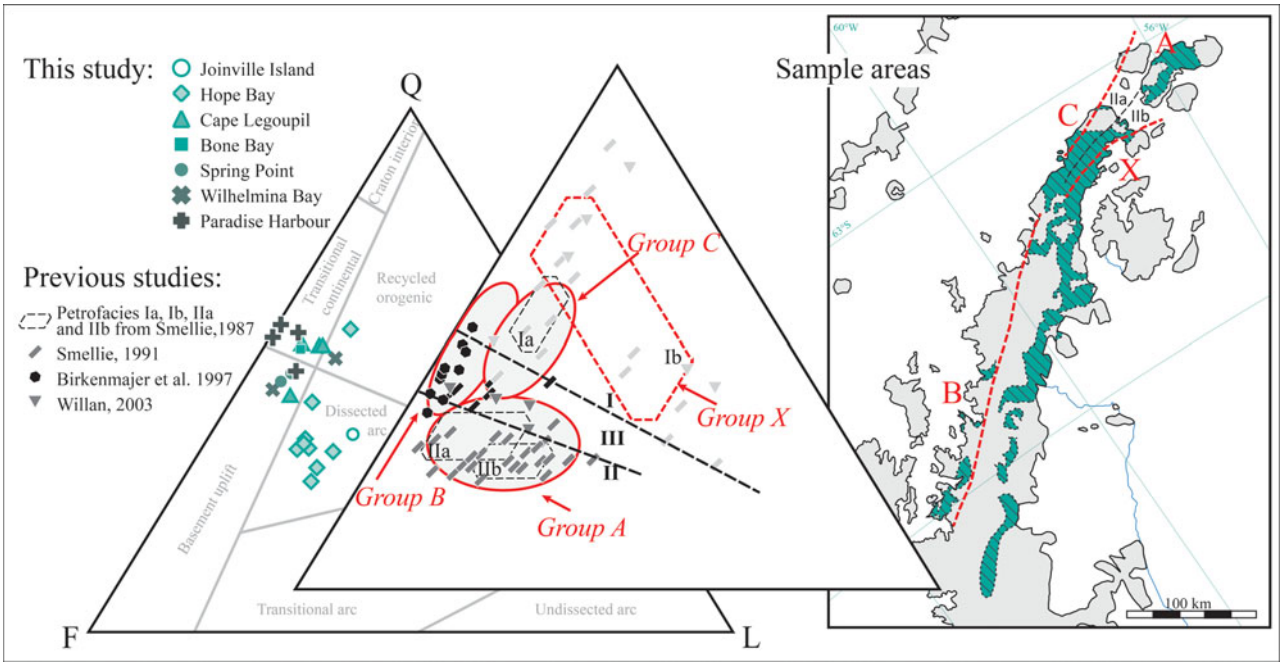

Figure 2. (Colour online) Modal composition of TPG sandstones (discrimination fields after Dickinson *et al.* 1983). Q – total quartz; F – total feldspar; L – lithic fragments. Right triangle shows data from Smellie (1987, 1991), Birkenmajer, Doktor & Swierczewska (1997), Willan (2003) and the compositional fields of the petrofacies I, II and III (dashed lines) proposed by Smellie (1991). Hexagonal dashed fields are petrofacies from Smellie (1987), but most of the samples from Smellie (1991) were included in Smellie (1987). Red areas are groups proposed in this study.

We have distinguished three distinct groups with different detrital modes and geographic allocations (Fig. 2). Group A correspond to samples from Hope Bay and Joinville Island with a higher content of lithic volcanic fragments. Group B have low amounts of lithic fragments and include samples from Paradise Harbour, Wilhelmina Bay, Charlotte Bay and Bone Bay. Finally Group C, samples from Cape Legoupil, have a content of lithic fragments between groups A and B, and a higher content of quartz. The modal composition in and between the groups is distributed continuously.

4.b. Whole-rock geochemistry

The major element composition suggests a felsic igneous origin for the detritus. The major elements

https://doi.org/10.1017/S0016756814000454 Published online by Cambridge University Press

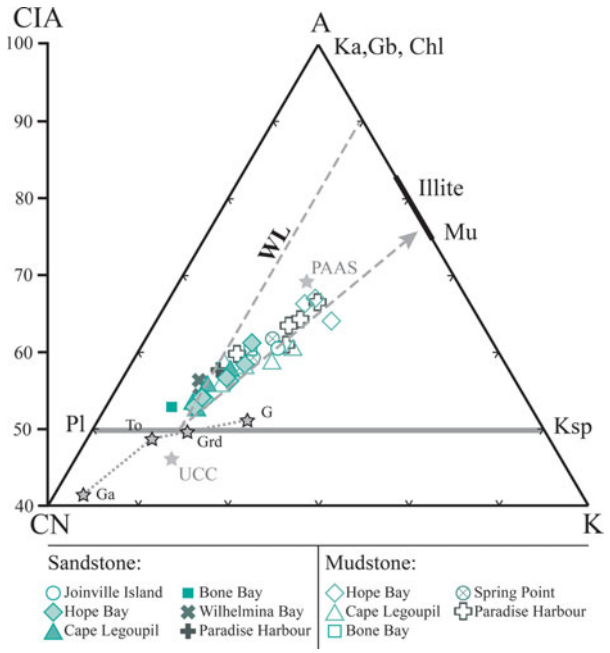

Figure 3. (Colour online) A–CN–K diagram (Nesbitt & Young, 1984), with indication of the weathering index CIA (chemical index of alteration; Nesbitt & Young, 1982). A – Al_2O_3; CN – $CaO^* + Na_2O$; K – K_2O. Ideal mineral compositions plotted are Ka – kaolinite; Gb – gibbsite; Chl – chlorite; Mu – muscovite; Pl – plagioclase; Ksp – K-feldspar; and illite. Typical igneous rock averages from Le Maitre (1976): Ga – gabbro; To – tonalite; Grd – granodiorite; G – granite. UCC – upper continental crust; PAAS – Post-Archaean Australian Shale. The solid horizontal line is the plagioclase–K-feldspar join. The dashed line parallel to the A–CN join is the predicted ideal feldspar weathering trend (WL) from granodiorite. The dashed arrowed line is the trend for the TPG.

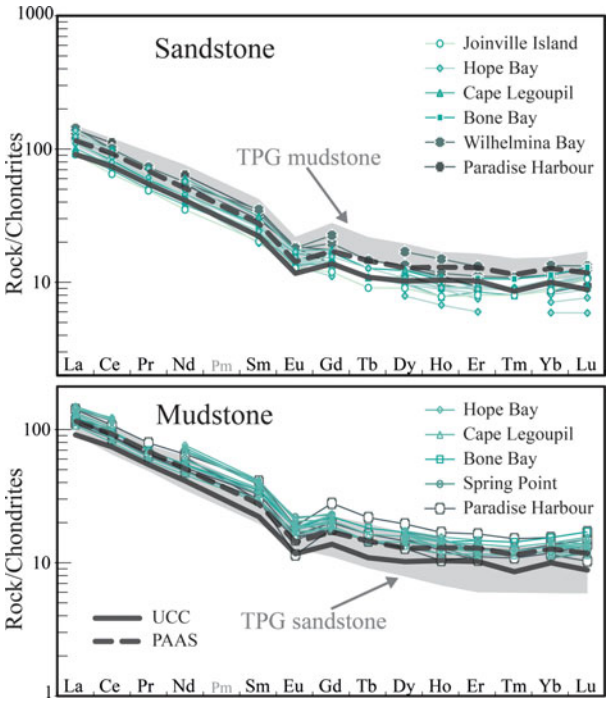

Figure 4. (Colour online) Chondrite-normalized REE compositions for the TPG sandstone and mudstone samples. UCC – average upper continental crust (McLennan, 2001); PAAS – Post-Archaean Australian Shale (Taylor & McLennan, 1985).

show a systematic geochemical contrast between the sandstone and mudstone samples (Table S1 in the online Supplementary Material available at http://journals.cambridge.org/geo). The SiO_2 and Na_2O contents are 70 ± 5 wt % and 3.6 ± 0.7 wt %, respectively, for the sandstone but only 65 ± 7 wt % and 2.6 ± 0.6 wt %, respectively, for the mudstone samples. Ti_2O, $Fe_2O_{3(T)}$, MgO and K_2O are positively correlated with Al_2O_3, and thus have higher average contents in the mudstone than in the sandstone samples (Table S1 in the online Supplementary Material available at http://journals.cambridge.org/geo). The remaining major oxides, CaO, MnO and P_2O_5, show no correlation with Al_2O_3. CaO contents are 1.2–1.8 wt % in both the sandstone and mudstone samples. MnO and P_2O_5 contents are lower in the sandstone than in the mudstone, except for the MnO content at Hope Bay, and P_2O_5 at Paradise Bay. Both the sandstone and mudstone samples have been affected by low to moderate degrees of chemical alteration, as indicated by the chemical index of alteration (CIA = 53–67; Nesbitt & Young, 1982), with the sandstone having lower values (CIA = 53–61) than the mudstone samples (CIA = 56–67). Samples in the A–CN–K plot (Fig. 3) present a linear trend, not parallel to the ideal weathering line (WL), which intersects the primary source composition of granodiorite to tonalite and trends towards muscovite.

The rare earth element (REE) composition is very similar to the average upper continental crust (McLennan, 2001) and the Post-Archaean Australian Shale (Taylor & McLennan, 1985). The mudstone samples have higher total REE abundances than the associated sandstone samples (Fig. 4). Compared to chondritic values, light REEs are enriched relative to heavy REEs as reflected by a La_N/Yb_N of 12.5 and 9.8 and Gd_N/Yb_N of 1.7 and 1.6 for the sandstone and mudstone samples, respectively. The Eu anomaly is negative with an average Eu/Eu^* of 0.78 and 0.67 in the sandstone and mudstone samples, respectively (Fig. 4).

In general, trace element contents of the mudstone samples are higher than for the sandstone samples (Table S1 in the online Supplementary Material available at http://journals.cambridge.org/geo). A positive correlation exists between trace elements and Al_2O_3 contents, reflecting the association of most trace elements with the clay fraction. This is particularly marked for Sc with 9.4 ± 2.7 and 14.5 ± 5.5 ppm, V with 86 ± 36 and 120 ± 50 ppm, Co with 10 ± 5 and 18 ± 7 ppm, Y with 23 ± 8 and 32 ± 9 ppm, Nb with 10 ± 2 and 17 ± 4 ppm, and Zn with 55 ± 26 and 95 ± 45 ppm for the sandstone and mudstone samples, respectively. Conversely, the mudstone samples are relatively depleted in Zr and Sr with 307 ± 211 and 165 ± 61 ppm, respectively, compared to the sandstone samples with 378 ± 134 and 244 ± 100 ppm, especially in the Paradise and Hope Bay rocks.

https://doi.org/10.1017/S0016756814000454 Published online by Cambridge University Press

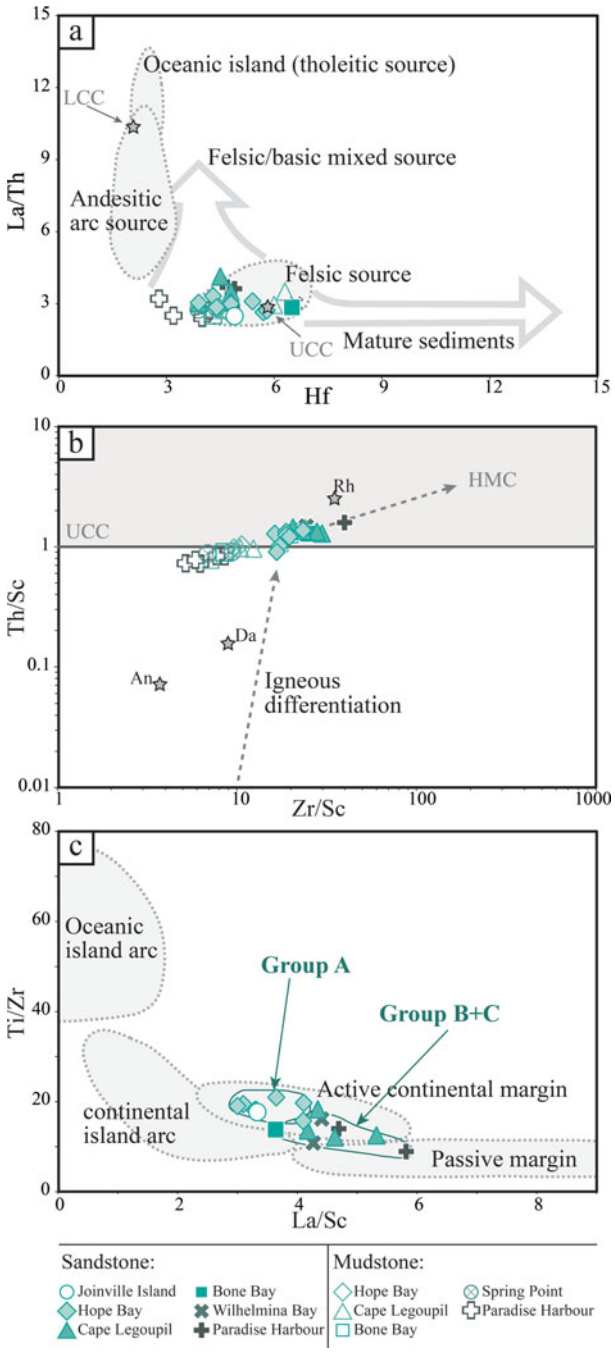

Figure 5. (Colour online) (a) La/Th v. Hf (discrimination fields from Floyd & Leveridge, 1987). LCC – lower continental crust; UCC – upper continental crust. (b) Th/Sc v. Zr/Sc (McLennan *et al.* 1993). UCC – upper continental crust; HMC – trend expected for heavy mineral sorting and concentration. Rock averages: An – andesite; Da – dacite; Rh – rhyolite. (c) Ti/Zr v. La/Sc sandstone diagram (Bhatia & Crook, 1986). The discrimination diagram is for sandstone.

Values of provenance-indicative elements in the sandstone samples, such as Th/Sc and La/Sc, range from 0.9 to 1.6 and 3.0 to 5.8, respectively, indicating an upper continental composition of the source (Fig. 5). The zircon and recycling indicator Zr/Sc is 16.3 to 39.9 in the sandstone and 5.2 to 23.4 in the mudstone samples. Differentiation between the sandstone and mudstone is marked in terms of the Zr/Sc ratio, with the sandstones having clearly higher ratios. Ti/Zr ranges from 8.9 to 20.9 in the sandstone and La/Th from 2.4 to 4.1 in the sandstone and mudstone samples. Sandstone samples from Group A have lower La/Sc and higher Ti/Zr than groups B and C, the latter plotting close to the boundary of the passive margin field (Fig. 5c). Sandstone samples from Group C have lower contents of $Fe_2O_{3(T)} + MgO$ wt %, TiO_2 wt % and Al_2O_3/SiO_2 than groups A and B (Table S1 in the online Supplementary Material available at http://journals.cambridge.org/geo), reflecting more maturity in those sediments, but Group B has a higher concentration of Zr.

4.c. Cathodoluminescence spectra of detrital quartz

According to the Augustsson & Reker (2012) discriminant colour diagram (Fig. 6), most quartz grains show typical blue and brown spectra. Bright and medium blue spectra have a higher intensity peak in the blue wavelength interval than in the red. On the other hand, dark blue and brown spectra have a slightly higher intensity in the red wavelength interval (Augustsson & Bahlburg, 2003; Augustsson & Reker, 2012). This is typical for a mixture of metamorphic and plutonic quartz. Felsic plutonic quartz grains make up 62 % of the total quartz grains measured, low-grade metamorphic or mafic plutonic quartz makes up 37 % and only 1 % have spectra typical for volcanic quartz (Fig. 7). Group A is dominated by felsic plutonic quartz grains with 86 % of the total quartz in this group, showing a trend ranging over the whole felsic plutonic region even extending a little into the mafic plutonic (or low-*T* metamorphic) region (Fig. 6a). Low-grade metamorphic or mafic plutonic quartz grains are more common in Group B with 71 % (Fig. 6b). Group C also displays the broad trend for plutonic quartz grains (Fig. 6c), medium blue being the most common CL colour, but with a larger proportion of the dark blue CL colour than in Group A.

Non-quartz-related additional peaks at *c*. 560 and 705 nm have been observed, especially in Group B. They reflect interference with neighbouring plagioclase or K-feldspar (see fig. 5 in Augustsson & Reker, 2012). This peak could affect the displayed spectra, especially for those grains that do not show strong luminescence (e.g. dark blue and brown). The proportion of quartz grains with dark CL colours could be underestimated in Group B. No grains with authigenic overgrowths have been observed.

5. Discussion

5.a. TPG petrofacies

Our petrographic results are similar to those of previous results reported by Smellie (1987, 1991), Birkenmajer (1992) and Willan (2003). Using this large amount of data from earlier studies we can define four petrofacies of which three were grouped in Section 4 above (Fig. 2).

https://doi.org/10.1017/S0016756814000454 Published online by Cambridge University Press

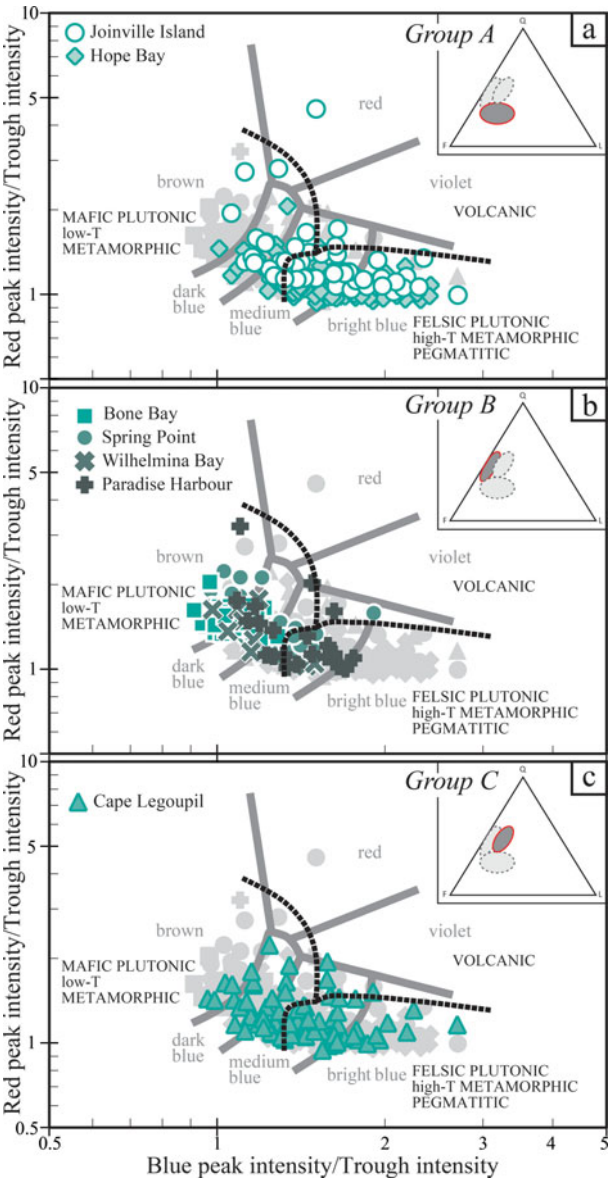

Figure 6. (Colour online) Relative peak intensities for measured quartz CL spectra (discrimination fields from Augustsson & Reker, 2012). (a) Petrofacies A. (b) Petrofacies B. (c) Petrofacies C.

Petrofacies A, B and C are defined from samples from groups A, B and C, respectively (Figs 1, 2). Petrofacies X, with high lithic and quartz contents, is not identified in our data, but it was recognized in the View Point area (Smellie, 1987, 1991; Willan, 2003).

The sandstone framework composition from petrofacies A is consistent with a dissected arc source (Fig. 2). This implies derivation from an eroded arc in which the plutonic roots had been exposed by erosion (Dickinson *et al.* 1983). The blue CL colour trend shown in Figure 6a suggests a plutonic origin for this petrofacies, but a high-*T* metamorphic origin should not be ruled out (Augustsson & Reker, 2012). Nevertheless, high contents of fresh feldspar and volcanic lithic fragments support the case for an igneous source. Volcanic quartz grains are practically absent in petrofacies A, even though the occurrence of volcanic fragments is unquestionable. For lithic felsic volcanic grains, the crystal size may be an important issue. The quartz phenocrysts observed in the volcanic fragments are too small to be measured by CL (< 130 μm) and for the more mafic volcanic fragments, quartz phenocrysts have not been observed.

Sediments from petrofacies B were derived from a continental block (Fig. 2), where erosion had exposed deeper levels of the continental crust (Dickinson *et al.* 1983). This petrofacies is dominated by low-grade metamorphic or dioritic quartz grains (Fig. 6b). However, it is clear that diorite can supply only a small amount of quartz, if any. The occurrence of more low-temperature metamorphic quartz, but the lack of an important metamorphic lithic content in this petrofacies, may reflect a grain-size issue. If the metamorphic rocks contain crystals in the range of sand sizes, as the quartz measured in this study does, they do not necessarily contain crystals of smaller sizes from which lithic fragments could be formed.

The combination of these data shows a contribution of magmatic and metamorphic sources. Hence, it is indeed possible that different parts of the same complex were eroded: a shallower plutonic-volcanic (petrofacies A) and a deeper plutonic-metamorphic (petrofacies B) source. In petrofacies C, the amount of quartz increases with respect to petrofacies A owing to its maturity (Fig. 2), showing recycling or a greater selection of grains and a longer transport pattern. Sediments from petrofacies C could have been deposited contemporaneously with deposition of petrofacies A, but in a distal basin, or it could represent the recycling of older sedimentary rocks.

Based on the quartz and feldspar ratio of previous TPG samples, Smellie (1987, 1991) distinguished three sandstone petrofacies (Fig. 2) and suggested a conceptual stratigraphic order: the Cape Legoupil and View Point formations followed by the Bahía Charlotte Formation, followed by the Hope Bay Formation. This model suggests that a volcanic-plutonic arc was being established on a pre-existing passive continental margin. In this case, the Cape Legoupil and View Point formations would represent the erosion of this passive margin, and the Hope Bay Formation, with more volcanic components, would represent the establishment of the arc. However, detrital U–Pb zircon patterns indicate that the Cape Legoupil Formation may be younger than the View Point Formation (Bradshaw *et al.* 2012), and has the same Permian principal component as the Hope Bay Formation (Barbeau *et al.* 2010). This indicates that the Permian igneous principal source was established previous to deposition of the Cape Legoupil Formation, or petrofacies C. Moreover, the lack of authigenic overgrowths around detrital quartz grains in petrofacies C suggests a first-cycle origin (e.g. Sanderson, 1984) as well as the fresh and angular feldspar grains, supporting a hypothesis of sorting and more distal deposition over reworking of an already existing older passive margin.

MacKinnon (1983) showed that during gradual erosion of a volcano-plutonic arc from an active

https://doi.org/10.1017/S0016756814000454 Published online by Cambridge University Press

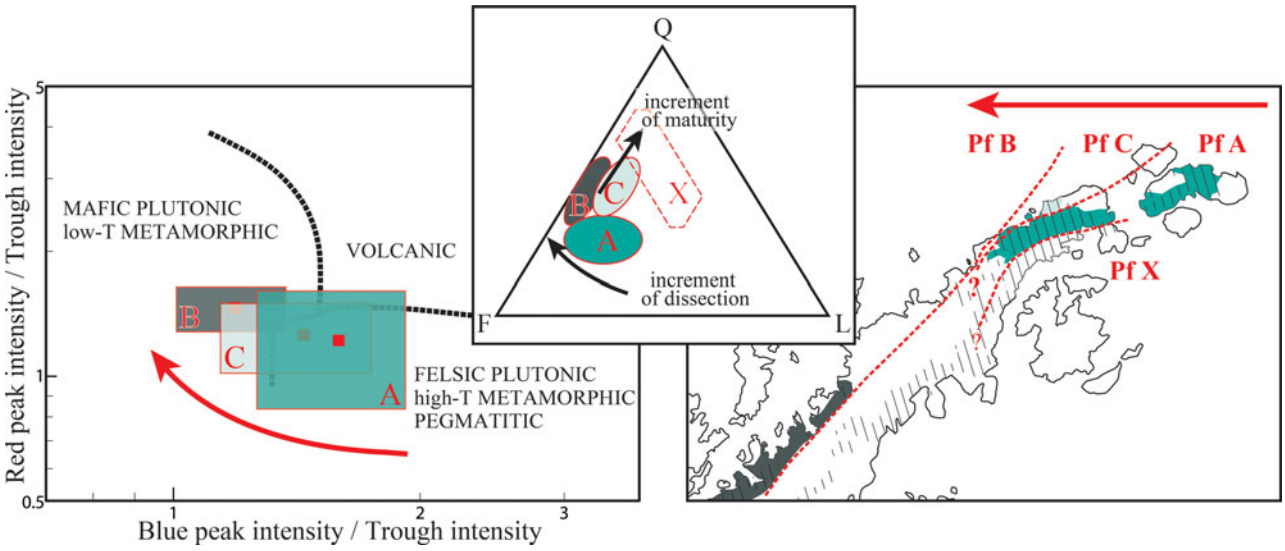

Figure 7. (Colour online) Petrofacies interpretation. Relative peak intensities for measured quartz CL spectra are plotted in mean values and first standard deviation fields for the three petrofacies. Arrows show the possible evolution from oldest to youngest petrofacies. The extension of the boundary for petrofacies B is speculative.

continental margin exhumation, the amount of lithic grains decreases progressively, similar to the trend between petrofacies A to B of the TPG (Fig. 2). MacKinnon's (1983) study is based on modal petrographic data from the Rakaia Group, New Zealand (which has similar characteristics to the TPG) using a well-determined fossil stratigraphy. In this particular case, after the decrease in lithic grains, there is an increase in sedimentary lithic fragments. He explains this feature as being due to the cannibalism of the same rising basin. However, in the TPG, petrofacies C does not show evidence of an increase in sedimentary lithic fragments, as would be expected for the cannibalism proposed by MacKinnon (1983).

Petrofacies X, with a recycled orogeny provenance (Fig. 2), was not sampled in this study. It does not follow the modal content trend of TPG petrofacies A, B and C, and has different U–Pb detrital zircon patterns. The matrix of conglomerates and clasts from View Point lack the typical Permian component of the TPG, implying that the deposition occurred before or shortly after the Carboniferous–Permian boundary (Bradshaw *et al.* 2012). Thus, petrofacies X was deposited before the establishment and erosion of the Permian magmatic source, probably in an older passive margin or in the early stage of development of an active setting. Unlike a passive margin, an active tectonic regime implies rapid exposure of potential source rocks; therefore, sediments are less affected by recycling and have a large proportion of zircons with ages close to the depositional age of sedimentation (Cawood, Hawkesworth & Dhuime, 2012). This is the case for petrofacies A, B and C. Furthermore, sandstones from View Point have detrital U–Pb zircon patterns with different age components, principally early Palaeozoic and Neoproterozoic (Bradshaw *et al*. 2012).

Here we suggest an evolution in the source area (a volcano-plutonic arc), reflected in the sedimentation of different petrofacies. Sediments from petrofacies A were deposited first, derived from the dissected arc. Petrofacies C represents a more distal deposition, probably contemporaneous with the older part of petrofacies A. Petrofacies B is the youngest deposit and is derived from the plutonic roots and deeper levels of the continental crust. Petrofacies X was likely derived from the erosion of an older passive margin and deposited before the other petrofacies. This evolution seems to be oriented from SE to NW in the Antarctic Peninsula (Fig. 7). Although there is no age control within the TPG, a westward subduction zone retreat has been suggested in the Permian period and Mesozoic era (Bradshaw *et al*. 2012).

5.b. Geochemical provenance signatures

Petrofacies A, B and C sediments were mainly fed by a felsic igneous source, typical of rocks derived from a silicic crystalline (plutonic-metamorphic) terrain with a lesser intermediate-acid volcanic component. The major element content, as shown in Figure 8 (Roser & Korsch, 1988), is indicative of a principal input from a primary felsic source, with an average composition ranging from tonalitic to granodioritic (Fig. 3). With increasing maturity, sediments plot progressively deeper in the P4 field of Roser & Korsch (1999), interpreted as recycling. In this study, samples from petrofacies C do not plot in the P4 field (Fig. 8), as expected for more-recycled sediments. On the other hand, the sandstones from Hope Bay that plot in P4 could indicate a local recycling and explain the higher quartz contained in this sample (Fig. 2)

Incompatible to compatible element ratios also indicate a felsic provenance (Fig. 5a) similar to the upper continental crust composition (Fig. 5b). La/Th reflects the influence of a magmatic arc in the hinterland (Bhatia, 1985; McLennan *et al.* 1993) and ratios such as

https://doi.org/10.1017/S0016756814000454 Published online by Cambridge University Press

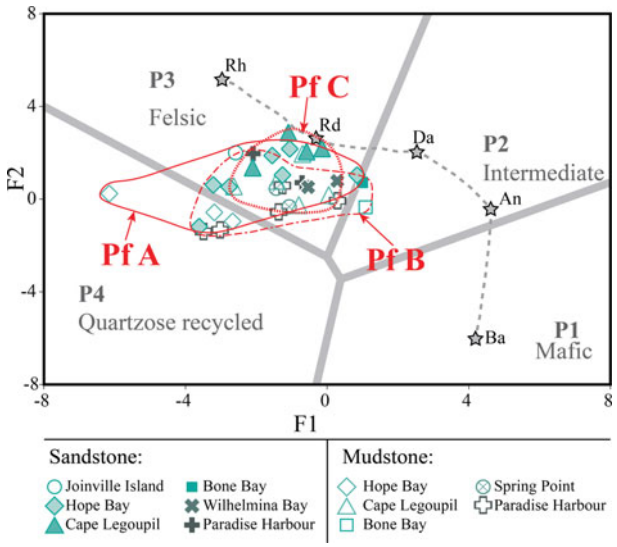

Figure 8. (Colour online) Provenance discriminant diagram (Roser & Korsch, 1988). P1 – mafic provenance; P2 – intermediate provenance; P3 – felsic provenance; and P4 – quartzose recycled provenance. Discrimination functions are $F1 = -1.773^{*}TiO_2 + 0.607^{*}Al_2O_3 + 0.76^{*}Fe_2O_{3T} - 1.5^{*}MgO + 0.616^{*}CaO + 0.509^{*}Na_2O - 1.224^{*}K_2O - 9.09$; $F2 = 0.445^{*}TiO_2 + 0.07^{*}Al_2O_3 - 0.25^{*}Fe_2O_{3T} - 1.142^{*}MgO + 0.438^{*}CaO + 1.475^{*}Na_2O + 1.426^{*}K_2O - 6.861$. Typical igneous rock averages from Le Maitre (1976): Rh – rhyolite; Rd – rhyodacite; Da – dacite; An – andesite; Ba – basalt.

La/Sc and Ti/Zr support the active continental margin provenance hypothesis (Fig. 5c). Differences within the petrofacies, such as a lower La/Sc in petrofacies A and lower $Fe_2O_{3(T)} + MgO\,\%$, $TiO_2\,\%$ and Al_2O_3/SiO_2 in petrofacies C, suggest a lesser contribution of volcanic rocks in petrofacies B and C and more maturity in petrofacies C.

The weathering pattern shown by TPG samples in the A–CN–K plot (Fig. 3) and relatively low CIA values attest to a low to moderate degree of source rock weathering (Fedo, Nesbitt & Young, 1995). This can indicate a cold and arid climate (cf. Nesbitt & Young, 1982). In a similar scenario, Willan (2003) suggested that the TPG was possibly derived from a glaciated continental margin. However, no textural evidence, such as striated clasts or dropstones, supports this interpretation (see discussion by Bradshaw *et al*. 2012). A glaciated continental margin would transport a wide range of continental materials from the Gondwana hinterland, but detrital zircons from the TPG are mostly Permian (Hervé, Miller & Pimpirev, 2005; Barbeau *et al.* 2010; Fanning *et al.* 2011). In addition to a cold, but not necessary glaciated, arid climate, rapid exhumation of the Permian source, erosion and proximal deposition could explain the low chemical weathering of TPG samples. Furthermore, the linear trend in the A–CN–K diagram and the separation of sandstone and mudstone samples suggests a tectonically active region, with dissection under non-steady-state weathering conditions (Nesbitt, Fedo & Young, 1997). The inclination of the TPG trend in Figure 3 relative to the ideal weathering line (WL) indicates that the variation in CIA cannot simply be accounted for by varying grain sizes and sorting. This feature suggests that the TPG samples have been affected by post-depositional K-metasomatism (Fedo, Nesbitt & Young, 1995).

Hydrodynamic separation of clay from sand-sized quartz and feldspar controls the REE distribution (Fig. 4). Also the Zr/Sc, Th/Sc, Ti/Zr and La/Sc ratios (Fig. 5; Table S1 in the online Supplementary Material at http://journals.cambridge.org/geo) are affected by the grain-size effect rather than recycling, which agrees with the immature textural characteristics. Separation between sandstone and mudstone samples, in terms of the Zr/Sc ratio (Fig. 5b), is indicative of higher zircon and heavy mineral concentrations in the TPG sandstone but it does not necessary reflect recycling. According to Morton (2012), the processes that have the greatest impact on heavy mineral accumulation are hydrodynamic sorting during transportation.

5.c. Palaeogeographic inferences

Contemporaneous sediments from Patagonia and New Zealand share similar characteristics with the TPG. The sediments could also be derived from volcanic-plutonic continental arcs prior to the Gondwana breakup, as part of the Palaeo-Pacific margin of Gondwana. Sedimentary rocks of the Duque de York Complex (DYC; part of the Madre de Dios Complex; Forsythe & Mpodozis, 1983) in Patagonia have the same dominant Permian zircon U–Pb peak (Hervé, Fanning & Pankhurst, 2003; Sepúlveda *et al.* 2010) and a similar sandstone framework composition (Faúndez, Hervé & Lacassie, 2002; Lacassie, Roser & Hervé, 2006; A. Quezada, unpub. Graduation thesis, Univ. Chile, 2010; Fig. 9). The Permian to lower Upper Triassic part of the Rakaia sub-terrane, in the New Zealand microcontinent, also has Permian zircon U–Pb peaks (Ireland, 1992; Pickard, Adams & Barley, 2000), and petrofacies equivalent to A and part of B (MacKinnon, 1983; Fig. 9)

In terms of geochemistry, the TPG, DYC and Rakaia rocks are also similar. The major element contents also indicate felsic sources (Roser & Korsch, 1999; Lacassie, Roser & Hervé, 2006). Similar matches are evident for the trace elements, although DYC samples have higher Zr/Sc (Lacassie, Roser & Hervé, 2006), indicative of greater zircon concentration, possibly due to longer transport or more intense weathering of the sand. CIA values of DYC sandstone and mudstone samples are higher than those of the TPG (Lacassie, Roser & Hervé, 2006) but they overlap the TPG CIA values. This suggests that the DYC was derived from a source with a comparable, although somewhat more severe, weathering regime. On the basis of the palynological record of the DYC, Sepúlveda *et al.* (2010) suggested a humid forest environment with an undergrowth of ferns for the DYC, contrasting with the cold and arid climate of the TPG based on CIA values. Although some palynological data from the TPG were recorded in the

https://doi.org/10.1017/S0016756814000454 Published online by Cambridge University Press

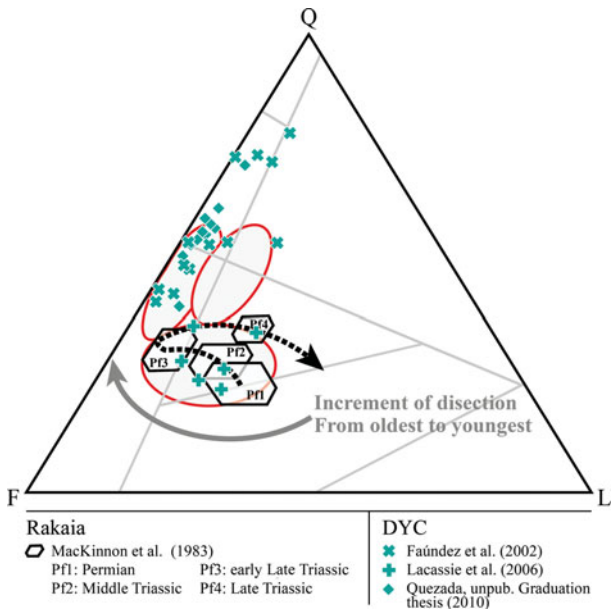

Figure 9. (Colour online) Modal composition of Duque de York Complex sandstone (Dickinson *et al.* 1983). Dashed arrowed line is the evolutionary trend of the Rakaia sub-terrane (MacKinnon, 1983). Hexagonal fields are Permian–Upper Triassic Rakaia petrofacies (MacKinnon, 1983). Grey arrowed line is the evolutionary trend of the TPG proposed in this study. Ellipses (red in online version) are the TPG petrofacies A, B and C as in Figure 7.

sixties, these data are contested and discounted now. CIA values from Rakaia sediments overlap those from the TPG and DYC (Roser & Korsch, 1999) and the slope of the respective trends are comparable, suggesting similar degrees of K-metasomatism and derivation from a primary source whose composition was in the tonalitic–granodioritic range.

Limestones and metabasalts are not common in the TPG. However, accreted Upper Carboniferous – Lower Permian limestone, metabasalt and chert are an important part in the Madre de Dios Accretionary Complex (Forsythe & Mpodozis, 1983). This assemblage suggests a subduction-related accretionary setting for the DYC (e.g. Hervé *et al.* 1981; Forsythe, 1982). Limestones associated with volcanic rocks have also been recognized in the Rakaia sub-terrane (MacKinnon, 1983), and studies of the depositional and deformational settings have favoured a fan depositional and accretionary wedge deformational model (Wandres *et al.* 2004 and references therein).

Major elements together with petrographic data (especially the presence of first-cycle quartz-feldspathic sand) support the idea that the petrofacies A, B and C of the TPG were deposited in a tectonic setting corresponding to an active continental margin. Active tectonics allow rapid discharge of sediments to the depocentre, and hence less weathering and chemical modification during transport, resulting in low CIA values. However, there is no clear evidence to suggest an accretionary complex origin for the TPG (Bradshaw *et al*. 2012; Smellie, 1987, 1991), unlike for the DYC (Hervé *et al.* 1981; Forsythe, 1982; Forsythe & Mpodozis, 1983). In this context, the TPG petrofacies A, B and C could have been deposited in a fore-arc basin, autochthonous to the Antarctic Peninsula (Bradshaw *et al*. 2012; Smellie, 1987, 1991), while the DYC was deposited on the subducted plate. In this configuration, the Rakaia sub-terrane could have had the same setting as the DYC, but only sharing the source in Permian to early Late Triassic times. In the Late Triassic, Rakaia sediments seem to have gone through increased recycling, with more sedimentary lithic components (MacKinnon, 1983; Roser & Korsch, 1999), not recorded in the DYC or TPG.

The DYC samples lack the corresponding petrofacies X of the TPG, but that part probably correlates with the Eastern Andes Metamorphic Complex (e.g. Bradshaw *et al.* 2012), northeast of the DYC in Patagonia. This complex is mostly Devonian to Carboniferous in age, but also has some younger parts with detrital zircon peaks of Carboniferous–Permian age (Hervé, Fanning & Pankhurst, 2003; Augustsson *et al.* 2006). Based on provenance considerations from petrographic and geochemical data, it has been suggested that the Eastern Andes Metamorphic Complex records deposition in a passive continental margin and was derived from a cratonic source (Faúndez, Hervé & Lacassie, 2002; Augustsson & Bahlburg, 2003). However, the Permian part of this complex (which crops out at the same latitude as the DYC but east of the Patagonian Batholith) shares similar U–Pb zircon patterns with petrofacies A, B and C of the TPG and the DYC. Augustsson *et al.* (2006) interpreted the differences in zircon populations from rocks of this complex as marking the change from a passive margin regime to the onset of eastward subduction and the development of a magmatic arc in the Late Carboniferous period in southern Patagonia. This is consistent with changes in the geochemical and petrological characteristics of sandstone samples from the same complex (Augustsson & Bahlburg, 2008). We interpret the differences in U–Pb detrital zircon patterns and petrography of petrofacies X and the rest of the TPG in the same way.

5.d. Location of the source: Antarctica or South America?

The combined petrographic, geochemical and the published geochronological data of the TPG (petrofacies A, B and C) and the DYC indicate that the sediments were mainly derived from a similar Permian volcanic-plutonic continental arc source which was relatively proximal to the depositional basin. Although the North Patagonian Massif and the Choiyoi volcanic province in north Patagonia are the most named sources for both complexes (e.g. Willan, 2003; Pankhurst *et al.* 2006; Fanning *et al.* 2011), this would imply a long transportation path, involving more sorting and sedimentary recycling. Riley, Flowerdew & Whitehouse (2012) and Millar, Pankhurst & Fanning (2002) have identified Permian magmatism coupled with metamorphic events in the basement of the Antarctic Peninsula. This implies

https://doi.org/10.1017/S0016756814000454 Published online by Cambridge University Press

a new proximal potential source for the TPG and suggests an extension of the early Palaeozoic continental margin magmatism from Patagonia (Riley, Flowerdew & Whitehouse, 2012).

The U–Pb detrital zircon patterns of the TPG and DYC (petrofacies A, B and C) samples indicate a strong input of Permian magmatic zircons, with age peaks ranging from *c*. 260 to 295 Ma for the TPG (Barbeau *et al.* 2010; Fanning *et al.* 2011), and 270 to 290 Ma for the DYC (Hervé, Fanning & Pankhurst, 2003; Sepúlveda *et al.* 2010). The Choiyoi magmatic province ranges from the arc-related magmatism (*c*. 281 Ma) of the Lower Choiyoi (Kleiman & Japas, 2009) to the intraplate post-orogenic suites of the Upper Choiyoi at *c*. 264 and *c*. 251 Ma (Rocha-Campos *et al*. 2011). Although the Choiyoi lacks the early Permian component of the DYC and TPG, Fanning *et al.* (2011) suggested, based on Lu–Hf isotope data in zircons, that the widespread Permian magmatism in the North Patagonian Massif (ages ranging from 295 to 257 Ma and extending to the Triassic; Pankhurst *et al.* 2006) could be regarded as a deeper extension of the Choiyoi, and that both areas are suitable sources for the TPG and DYC.

One of the most widely accepted palaeogeographic reconstructions locates the Antarctic Peninsula west of Patagonia in Middle Jurassic time (König & Jokat, 2006). However, this reconstruction implies a long overlap between Patagonia and the Antarctic Peninsula, and the DYC would have been accreted to the Antarctic Peninsula. These may indicate that there was a smaller degree of overlap, or a 'short-legged tango' configuration (Miller, 2007) during Permian and Triassic times or at least during Late Triassic time when the Madre de Dios Accretionary Complex accreted to the fore-arc (Willner *et al.* 2009). If northern Patagonia was the principal source of the TPG and DYC, this would imply long transport patterns of the sediments, which is not found in the textural characteristics of the detritus. Ramos (2008) proposed an extension of the Permian magmatism further to the south (present coordinates) in his 'western magmatic belt', even though no upper Palaeozoic crystalline rocks are exposed in southernmost Patagonia. According to Pankhurst *et al.* (2006), Permian magmatism is the result of the collision of the Deseado block and a following break-off of the slab under the North Patagonian Massif. In this model, no prolongation of this Permian magmatism into southern Patagonia or the Antarctic Peninsula is allowed. However, Hervé *et al.* (2010) reported low Th–U metamorphic Permian zircons in migmatitic gneiss within drill cores in the Magallanes Basin. In the Antarctic Peninsula, Permian magmatism, with age peaks at *c*. 255, 260 and 275 Ma, is coupled with similar high-grade metamorphism and migmatization (Millar, Pankhurst & Fanning, 2002; Riley, Flowerdew & Whitehouse, 2012). In Tierra del Fuego, Hervé *et al.* (2010) suggested at least 8 to 12 km of erosion before deposition of Middle–Late Jurassic volcanic rocks, which would be an important source of detritus. However, no Permian metamorphic zircons have been reported yet for the TPG and DYC.

With the available data it is difficult to discern whether the magmatism of the Choiyoi–North Patagonian Massif extended into Tierra del Fuego and the Antarctic Peninsula or whether they were different but contemporaneous magmatic events. The North Patagonian Massif and the Choiyoi lack the high-grade Permian metamorphic event (no development of metamorphic zircons) which occurred in Tierra del Fuego and the Antarctic Peninsula, and have an early Permian component not yet reported in the Antarctic Peninsula crystalline basement. A key element is the Deseado Massif, which is located between the North Patagonian Massif and Tierra del Fuego. This block is characterized by weathered and altered granitoids of Silurian and Devonian age intruding into Neoproterozoic metasedimentary rocks (Pankhurst *et al.* 2003), which differs from the Cambrian basement of Tierra del Fuego (Hervé *et al.* 2010; Pankhurst *et al.* 2003; Sölner, Miller & Hervé, 2000). However, basement rocks are poorly exposed in this area and it is possible that Permian igneous rocks lie hidden beneath younger sedimentary or volcanic rocks.

6. Conclusions

Our results, in combination with published data, permit the identification of different petrofacies, with compositional changes that may record the uplift and exposure of a volcano-plutonic continental arc. This source was located relatively close to the depositional basin and has a tonalitic to granodioritic composition. Deep erosion allowed the exposure of the plutonic-metamorphic basement. Despite this, the chemical weathering in the source area was low, suggesting a rapid exhumation in a dry and cold climate.

The volcano-plutonic arc was likely located along the active Gondwana continental margin, probably in the south Patagonia – Antarctic Peninsula sector. This source could contribute detritus to other sedimentary sequences such as the DYC in southern Patagonia, as indicated by the strong chemical, petrographic and chronological similarities between those sediments.

In this case study, a combination of petrographic, geochemical and cathodoluminescence of quartz provenance analyses were used to identify petrofacies and reconstruct the depositional setting of the TPG. Given the lack of stratigraphic information, this interpretation would not have been possible without the combination of different methods, highlighting the importance of using multiple tools for provenance analysis.

Acknowledgements. This work was supported by the Anillo Antártico ART-105 and Inach B-01–08 projects. Special thanks to the crew of the Almirante Oscar Viel, Leucoton, Lautaro and Aquiles from the Chilean Navy and Thomas Haber, Fernando Poblete, Manfred Brix, Alain Demant, Mark Fanning, Carolina Guzmán and Millarca Valenzuela for

participating in the field work and discussion. Stefan Kraus is acknowledged for rock samples and Matthew Callaghan for checking the English grammar. Two anonymous reviewers are acknowledged for comments that improved the paper.

Supplementary material

To view supplementary material for this article, please visit http://dx.doi.org/10.1017/S0016756814000454.

References

ALARCÓN, B., AMBRUS, J., OLCAY, L. & VIEIRA, C. 1976. Geología del Estrecho de Gerlache entre los paralelos 64° y 65° lat. Sur, Antártica Chilena. *Serie Científica del Instituto Antártico Chileno* **4**, 7–51.

AUGUSTSSON, C. & BAHLBURG, H. 2003. Cathodoluminescence spectra of detrital quartz as provenance indicators for Paleozoic metasediments in southern Andean Patagonia. *Journal of South American Earth Sciences* **16**, 15–26.

AUGUSTSSON, C. & BAHLBURG, H. 2008. Provenance of late Palaeozoic metasediments of the Patagonia proto-Pacific margin (southernmost Chile and Argentina). *International Journal of Earth Sciences (Geologische Rundschau)* **97**, 71–88.

AUGUSTSSON, C., MÜNKER, C., BAHLBURG, H. & FANNING, C. M. 2006. Provenance of late Palaeozoic metasediments of the SW South American Gondwana margin: a combined U–Pb and Hf-isotope study of single detrital zircons. *Journal of the Geological Society, London* **163**, 983–95.

AUGUSTSSON, C. & REKER, A. 2012. Cathodoluminescence spectra of quartz as provenance indicators revisited. *Journal of Sedimentary Research* **82**, 559–70.

BARBEAU, D. L., DAVIS, J. T., MURRAY, K. E., VALENCIA, V., GEHRELS, G. E., ZAHID, K. M. & GOMBOSI, D. J. 2010. Detrital-zircon geochronology of the metasedimentary rocks of northwestern Graham Land. *Antarctic Science* **22**, 65–78.

BHATIA, M. R. 1985. Composition and classification of Palaeozoic flysch mudrocks of eastern Australia: implications in provenance and tectonic setting interpretation. *Sedimentary Geology* **41**, 249–68.

BHATIA, M. R. & CROOK, K. A. W. 1986. Trace element characteristics of greywackes and tectonic setting discrimination of sedimentary basins. *Contributions to Mineralogy and Petrology* **92**, 181–93.

BIRKENMAJER, K. 1992. Trinity Peninsula Group (Permo-Triassic) at Paradise Harbour, Antarctic Peninsula. *Studia Geologica Polonica* **101**, 7–25.

BIRKENMAJER, K., DOKTOR, M. & SWIERCZEWSKA, A. 1997. A turbidite sedimentary log of the Trinity Peninsula Group (?Upper Permian-Triassic) at Paradise Harbour, Danco Coast (Antarctic Peninsula): sedimentology and petrology. *Studia Geologica Polonica* **110**, 61–90.

BRADSHAW, J. D., VAUGHAN, A. P. M., MILLAR, I. L., FLOWERDEW, M. J., TROUW, R. A. J., FANNING, C. M. & WHITEHOUSE, M. J. 2012. Permo-Carboniferous conglomerates in the Trinity Peninsula Group at View Point, Antarctic Peninsula: sedimentology, geochronology and isotope evidence for provenance and tectonic setting in Gondwana. *Geological Magazine* **149**, 626–44.

BRITISH ANTARCTIC SURVEY. 1985. *Northern Graham Land and the South Shetland Islands Geological Map. 1:500.000. Series BAS 500G, Sheet 2, Edition 1*. Cambridge: British Antarctic Survey.

CAWOOD, P. A., HAWKESWORTH, C. J. & DHUIME, B. 2012. Detrital zircon record and tectonic setting. *Geology* **40**, 875–78.

DALZIEL, I. W. D. 1984. *Tectonic Evolution of a Forearc Terrane, Southern Scotia Ridge, Antarctica*. Geological Society of America Special Paper 200, 32 pp.

DICKINSON, W. R., BEARD, L. S., BRAKENRIDGE, G. R., ERJAVEC, J. L., FERGUSON, R. C., INMAN, K. F., KNEPP, R. A., LINDBERG, F. A. & RYBERG, P. T. 1983. Provenance of North American Phanerozoic sandstones in relation to tectonic setting. *Geological Society of America Bulletin* **94**, 222–35.

FANNING, C. M., HERVÉ, F., PANKHURST, R. J., RAPELA, C. W., KLEIMAN, L. E., YAXLEY, G. M. & CASTILLO, P. 2011. Lu-Hf isotope evidence for the provenance of Permian detritus in accretionary complexes of western Patagonia and the northern Antarctic Peninsula region. *Journal of South American Earth Sciences* **32**, 485–96.

FAÚNDEZ, V., HERVÉ, F. & LACASSIE, J. P. 2002. Provenance and depositional setting of pre-Late Jurassic turbidite complexes in Patagonia, Chile. *New Zealand Journal of Geology and Geophysics* **45**, 411–25.

FEDO, C. M., NESBITT, H. W. & YOUNG, G. M. 1995. Unravelling the effects of potassium metasomatism in sedimentary rocks and paleosols, with implications for paleoweathering conditions and provenance. *Geology* **23**, 921–4.

FLOWERDEW, M. J. 2008. Short Note: On the age and relation between metamorphic gneisses and the Trinity Peninsula Group, Bowman Coast, Graham Land, Antarctica. *Antarctic Science* **20**, 511–2.

FLOYD, P. A. & LEVERIDGE, B. E. 1987. Tectonic environment of the Devonian Gramscatho basin, south Cornwall: framework mode and geochemical evidence from turbiditic sandstones. *Journal of the Geological Society, London* **144**, 531–42.

FOLK, R. L. 1980. *Petrology of Sedimentary Rocks*. Hemphill, 159 pp.

FORSYTHE, R. 1982. The late Palaeozoic to early Mesozoic evolution of southern South America: a plate tectonic interpretation. *Journal of the Geological Society, London* **139**, 671–82.

FORSYTHE, R. D. & MPODOZIS, C. 1983. Geología del Basamento pre-Jurásico Superior en el Archipiélago Madre de Dios, Magallanes, Chile. *Servicio Nacional de Geología y Minería, Boletín* **39**, 1–63.

GHIDELLA, M. E., LAWVER, L. A., MARENSSI, S. & GAHAGAN, L. M. 2007. Modelos de cinemática de placas para Antártida durante la ruptura de Gondwana: una revisión. *Revista Asociación Geológica Argentina* **62**, 636–46.

GHIDELLA, M. E., YÁÑEZ, G. & LABRECQUE, J. L. 2002. Revised tectonic implications for the magnetic anomalies of the western Weddell Sea. *Tectonophysics* **347**, 65–86.

HERVÉ, F. 1993. Palaeozoic metamorphic complexes in the Andes of Aysen, southern Chile (west of ?Occidentalia). In *Proceedings of the First Circum-Pacific and Circum-Atlantic Terrane Conference* (eds F. Ortega-Gutiérrez, P. Coney, E. Centeno-García & A. Gomez-Caballero), pp. 64–5. Guanajuato, Mexico.

HERVÉ, F., CALDERÓN, M., FANNING, C. M., KRAUS, S. & PANKHURST, R. J. 2010. SHRIMP chronology of the Magallanes Basin basement, Tierra del Fuego: Cambrian plutonism and Permian high-grade metamorphism. *Andean Geology* **37**, 253–75.

HERVÉ, R., DAVIDSON, J., GODOY, E., MPODOZIS, C. & COVACEVICH, V. 1981. The Late Paleozoic in Chile:

stratigraphy, structure and possible tectonic framework. *Anais da Academia Brasileira de Ciências* **53**, 362–73.

HERVÉ, F., FANNING, C. M. & PANKHURST, R. J. 2003. Detrital zircon age patterns and provenance of the metamorphic complexes of southern Chile. *Journal of South American Earth Sciences* **16**, 107–23.

HERVÉ, F., MILLER, H. & PIMPIREV, C. 2005. Patagonia-Antarctica connections before Gondwana break-up. In *Antarctica: Contribution to Global Earth Sciences* (eds D. K. Fütterer, D. Damaske, G. Kleinschmidt, H. Miller & F. Tessensohn), pp. 217–28. Berlin, Heidelberg, New York: Springer-Verlag.

HYDEN, G. & TANNER, P. W. G. 1981. Late Paleozoic-Early Mesozoic fore-arc basin sedimentary rocks at the Pacific margin in Western Antarctica. *Geologische Rundschau* **70**, 529–41.

IRELAND, T. R. 1992. Crustal evolution of New Zealand: evidence from age distribution of detrital zircons in Western Province paragneisses and Torlesse graywacke. *Geochimica et Cosmochimica Acta* **56**, 911–20.

INGERSOLL, R. V., FULLARD, T. F., FORD, R. D., GRIMM, J. P., PICKLE, J. D. & SARES, S. W. 1984. The effect of grain size on detrital modes: a test of the Gazzi-Dickinson point counting method. *Journal of Sedimentary Petrology* **54**, 103–16.

KLEIMAN, L. E. & JAPAS, M. S. 2009. The Choiyoi volcanic province at 34 °S–36 °S (San Rafael, Mendoza, Argentina): implications for the Late Palaeozoic evolution of the southwestern margin of Gondwana. *Tectonophysics* **473**, 283–99.

KÖNIG, M. & JOKAT, W. 2006. The Mesozoic breakup of the Weddell Sea. *Journal of Geophysical Research* **111**, 1–28.

LACASSIE, J. P., ROSER, B. P. & HERVÉ, F. 2006. Sedimentary provenance study of the post-Early Permian to pre-Early Cretaceous metasedimentary Duque de York Colmes, Chile. *Revista Geológica de Chile* **33**, 199–219.

LE MAITRE, R. W. 1976. The chemical variability of some common igneous rocks. *Journal of Petrology* **17**, 589–637.

MACKINNON, T. C. 1983. Origin of the Torlesse terrane and coeval rocks, South Island, New Zealand. *Geological Society of America Bulletin* **93**, 625–34.

MCLENNAN, S. M. 2001. Relationships between the trace element composition of sedimentary rocks and upper continental crust. *Geochemistry, Geophysics, Geosystems* **2**, 1–24.

MCLENNAN, S. M., HEMMING, S., MCDANIEL, D. K. & HANSON, G. N. 1993. Geochemical approaches to sedimentation, provenance and tectonics. In *Processes Controlling the Composition of Clastic Sediments* (eds M. J. Johnnson & A. Basu), pp. 21–40. Geological Society of America Special Papers no. 285.

MILLER, H. 2007. History of views on the relative positions of Antarctica and South America: a 100-year tango between Patagonia and the Antarctic Peninsula. In *Antarctica: A Keystone in a Changing World – Online Proceedings of the 10th ISAES* (eds A. K. Cooper & C. R. Raymond), 4 pp. USGS Open-File Report 2007–1047, Short Research Paper 41.

MILLAR, I. L., PANKHURST, R. J. & FANNING, C. M. 2002. Basement chronology of the Antarctic Peninsula: recurrent magmatism and anatexis in the Palaeozoic Gondwana margin. *Journal of Geological Society, London* **159**, 145–57.

MORTON, A. 2012. Value of heavy minerals in sediments and sedimentary rocks for provenance, transport history and stratigraphic correlation. In *Short Course Volume 42: Quantitative Mineralogy and Microanalysis of Sediments and Sedimentary Rocks* (ed. P. Sylvester), pp. 133–65. Mineralogical Association of Canada.

NESBITT, H. W., FEDO, C. M. & YOUNG, G. M. 1997. Quartz and feldspar stability, steady and non-steady state weathering, and petrogenesis of siliciclastic sands and muds. *Journal of Geology* **105**, 173–91.

NESBITT, H. W. & YOUNG, G. M. 1982. Early Proterozoic climates and plate motions inferred from mayor element chemistry of lutites. *Nature* **199**, 715–7.

NESBITT, H. W. & YOUNG, G. M. 1984. Prediction of some weathering trends of plutonic and volcanic rocks based on thermodynamic and kinetic considerations. *Geochimica et Cosmochimica Acta* **48**, 1523–34.

PANKHURST, R. J., RAPELA, C. W., FANNING, C. M. & MÁRQUEZ, M. 2006. Gondwanide continental collision and the origin of Patagonia. *Earth-Science Reviews* **76**, 235–57.

PANKHURST, R. J., RAPELA, C. W., LOSKE, W. P., MÁRQUEZ, M. & FANNING, C. M. 2003. Chronological study of the pre-Permian basement rocks of southern Patagonia. *Journal of South American Earth Sciences* **16**, 27–44.

PICKARD, A. L., ADAMS, C. J. & BARLEY, M. E. 2000. Australian provenance for Upper Permian to Cretaceous rocks forming accretionary complexes on the New Zealand sector of the Gondwanaland margin. *Australian Journal of Earth Sciences* **47**, 987–1007.

POBLETE, F., ARRIAGADA, C., ROPERCH, P., ASTUDILLO, N., HERVÉ, F., KRAUS, S. & Le ROUX, J. P. 2011. Paleomagnetism and tectonics of the South Shetland Islands and the northern Antarctic Peninsula. *Earth and Planetary Science Letters* **302**, 299–313.

RAMOS, V. A. 2008. Patagonia: a Paleozoic continent adrift? *Journal of South American Earth Sciences* **26**, 235–51.

RILEY, T. R., FLOWERDEW, M. J. & WHITEHOUSE, M. J. 2012. U-Pb ion-microprobe zircon geochronology from the basement inliers of eastern Graham Land, Antarctic Peninsula. *Journal of the Geological Society, London* **169**, 381–93.

ROCHA-CAMPOS, A. C., BASEI, M. A., NUTMAN, A. P., KLEIMAN, L. E., VARELA, R., LLAMBIAS, E., CANILE, F. M. & DA ROSA, O. C. R. 2011. 30 million years of Permian volcanism recorded in the Choiyoi igneous province (W Argentina) and their source for younger ash fall deposits in the Paraná Basin: SHRIMP U-Pb zircon geochronology evidence. *Gondwana Research* **19**, 509–23.

ROSER, B. P. & KORSCH, R. J. 1988. Provenance signatures of sandstone-mudstone suites determined using discriminant function analysis of major-element data. *Chemical Geology* **67**, 119–39.

ROSER, B. P. & KORSCH, R. J. 1999. Geochemical characterization, evolution and source of a Mesozoic accretionary wedge: the Torlesse terrane, New Zealand. *Geological Magazine* **136**, 493–512.

SANDERSON, I. D. 1984. Recognition and significance of inherited quartz overgrowths in quartz arenites. *Journal of Sedimentary Petrology* **54**, 473–86.

SEPÚLVEDA, F. A., PALMA-HELDT, S., HERVÉ, F. & FANNING, C. M. 2010. Constraints for the depositional age of the Duque de York Complex in the allochthonous Madre de Dios Terrane, southern Chile: first palynological record and palaeoclimatic implications. *Andean Geology* **37**, 375–97.

SMELLIE, J. L. 1987. Sandstone detrital modes and basinal setting of the Trinity Peninsula Group, northern Graham Land, Antarctic Peninsula: a preliminary survey. In

Gondwana VI: Structure, Tectonics and Geophysics (ed. G. D. McKenzie), pp. 199–207. American Geophysical Union, Geophysical Monograph vol. 40. Washington, DC, USA.

SMELLIE, J. L. 1991. Stratigraphy, provenance and tectonic setting of (?)Late Palaeozoic-Triassic sedimentary sequences in northern Graham Land and South Scotia Ridge. In *Geological Evolution of Antarctica* (eds M. R. A. Thomson, J. A. Crame & J. W. Thomson), pp. 411–7. Cambridge University Press.

SMELLIE, J. L. & MILLAR, I. L. 1995. New K-Ar isotopic ages of schists from Nordenskjold Coast, Antarctic Peninsula: oldest part of the Trinity Peninsula Group? *Antarctic Science* **7**, 191–96.

SMELLIE, J. L., ROBERTS, B. & HIRONS, S. R. 1996. Very low- and low-grade metamorphism in the Trinity Peninsula Group (Permo-Triassic) of northern Graham Land, Antarctic Peninsula. *Geological Magazine* **133**, 583–94.

SÖLNER, F., MILLER, H. & HERVÉ, M. 2000. An Early Cambrian granodiorite age from the pre-Andean basement of Tierra del Fuego (Chile): the missing link between South America and Antarctica? *Journal of South American Earth Sciences* **13**, 163–77.

STOREY, B. C. & GARRETT, S. W. 1985. Crustal growth of the Antarctic Peninsula by accretion, magmatism and extension. *Geological Magazine* **122**, 5–14.

TAYLOR, S. R. & MCLENNAN, S. M. 1985. *The Continental Crust: Its Composition and Evolution*. Oxford: Blackwell Scientific Publications, 312 pp.

THOMSON, M. R. A. 1975. First marine Triassic fauna from the Antarctic Peninsula. *Nature* **257**, 577–8.

VAUGHAN, A. P. M. & STOREY, B. C. 2000. The eastern Palmer Land shear zone: a new terrane accretion model for the Mesozoic development of the Antarctic Peninsula. *Journal of the Geological Society, London* **157**, 1243–56.

WANDRES, A. M. C., BRADSHAW, J. D., WEAVER, S. D., MAAS, R., IRELAND, T. R. & EBY, G. N. 2004. Provenance of the sedimentary Rakaia sub-terrane, South Island, New Zealand: the use of igneous clast compositions to define the source. *Sedimentary Geology* **168**, 193–226.

WILLAN, R. C. R. 2003. Provenance of Triassic-Cretaceous sandstones in the Antarctic Peninsula: implications for terrane models during Gondwana breakup. *Journal of Sedimentary Research* **73**, 1062–77.

WILLNER, A. P., SEPÚLVEDA, F. A., HERVÉ, F., MASSONNE, H.-J. & SUDO, M. 2009. Conditions and timing of pumpellyite-actinolite-facies metamorphism in the Early Mesozoic frontal accretionary prism of the Madre de Dios Archipelago (Latitude 50° 20' S; Southern Chile). *Journal of Petrology* **50**, 2127–55.